COMMUNICATION

Multistable Architected Materials for Trapping Elastic Strain Energy

*Sicong Shan, Sung H. Kang, Jordan R. Raney, Pai Wang, Lichen Fang, Francisco Candido, Jennifer A. Lewis, and Katia Bertoldi**

We combine 3D printing and numerical analysis to design a new class of architected materials that exhibits controlled trapping of elastic energy. These programmed structures contain beam elements with geometries that are specifically designed to enable large, local bistable deformations. When these materials are mechanically deformed, the beams locally reconfigure into a higher-energy, yet stable, deformed state, akin to a phase transformation. The energy applied during deformation, whether via low rate quasistatic loading or via impact tests, can be stored in this manner until a sufficient reverse force is applied that allows the deformed beams to return to their original configuration. The mechanism of energy absorption stems solely from the structural geometry of the printed beam elements, and is therefore both materials- and loading rate- independent. These architected materials offer a new strategy for significantly enhancing energy absorption.

Energy-absorbing materials are widely deployed for personnel protection, crash mitigation in automobiles and aircraft, and protective packaging of delicate components. Many strategies have been investigated to create materials that efficiently dissipate mechanical energy, including plastic deformation in metals,[1–4] fragmentation in ceramics,[5] and rate-dependent viscous processes.[1,6,7] However, in all of these systems there are challenges associated with either reusability or rate dependency. Most recently, mechanical metamaterials have been fabricated in novel geometries to realize recoverable energy-absorbing behavior in elastic systems,[8–11] suggesting novel strategies for mechanical dissipation of energy.

Dr. S. Shan, Prof. S. H. Kang, Dr. J. R. Raney, P. Wang, L. Fang, F. Candido, Prof. J. A. Lewis, Prof. K. Bertoldi
School of Engineering and Applied Sciences
Harvard University
Cambridge, MA 02138, USA
E-mail: bertoldi@seas.harvard.edu
Prof. S. H. Kang
Department of Mechanical Engineering and Hopkins Extreme Materials Institute
Johns Hopkins University
Baltimore, MD 21218, USA
Dr. J. R. Raney, Prof. J. A. Lewis
Wyss Institute for Biologically Inspired Engineering
Harvard University
Cambridge, MA 02138, USA
Prof. K. Bertoldi
Kavli Institute for Bionano Science and Technology
Harvard University
Cambridge, MA 02138, USA

DOI: 10.1002/adma.201501708

Here, we report a new class of architected materials in which the energy inserted into a system during loading is trapped in the form of elastic deformation of a large number of bistable elastic beams. Using direct ink writing,[12] an extrusion-based 3D printing method, we rapidly fabricate customized energy-absorbing architectures. Their design, which is inspired by the exotic response of bistable elastic elements,[13–18] is guided by numerical finite element (FE) simulations. Importantly, the energy-trapping mechanism depends solely on the (reversible) change in state of prescribed structural geometries. Hence, the mechanical response is reversible and repeatable, and independent of scale, rate, and loading history. Remarkably, these architected materials reduce the peak acceleration and forces experienced during impact by an order of magnitude compared to previously proposed mechanisms that exploit only snap-through instabilities.[10]

To illustrate the proposed mechanism, we consider an elastic constrained tilted beam. In contrast to a vertical elastic beam that buckles under axial compression, but fully recovers its initial shape when unloaded (**Figure 1**a), a tilted beam may snap between two different stable configurations[19–22] and retain its deformed shape after unloading (Figure 1b). Interestingly, such a bistable tilted beam is capable of locking in most of the energy inserted into the system during loading (quantified by the shaded area under the corresponding force–displacement curve), indicating that it can be used as an energy absorbing element.

To create energy trapping architected materials that exploit the bistability of tilted elastic beams, it is necessary to accurately control structural features. Direct ink writing offers a facile method for rapidly fabricating materials composed of arrays of tilted elastic beams in programmable motifs. With this 3D printing technique, viscoelastic inks are extruded through fine deposition nozzles in a layer-by-layer manner.[23–25] The inks exhibit shear-thinning behavior, which facilitates their flow through the nozzle during printing, as well as a shear elastic modulus that ensures that the printed features are self-supporting. Specifically, we used a polydimethylsiloxane (PDMS) ink to print energy-trapping, architected materials (Figures S1 and S2, Supporting Information). This silicone-based ink maintains its structural integrity prior to cross-linking the printed structures at 100 °C for 30 min to yield an elastomeric material with an initial shear modulus μ_0 = 0.32 MPa (Figure S3, Supporting Information). We note that direct ink writing is particularly well-suited to our beam-based geometries, since narrow features with tunable aspect ratios can be readily fabricated by locally varying the print velocity. Additionally, certain common defects, such as poorly connected nodes, are prevented by printing a structure from one continuous filament.

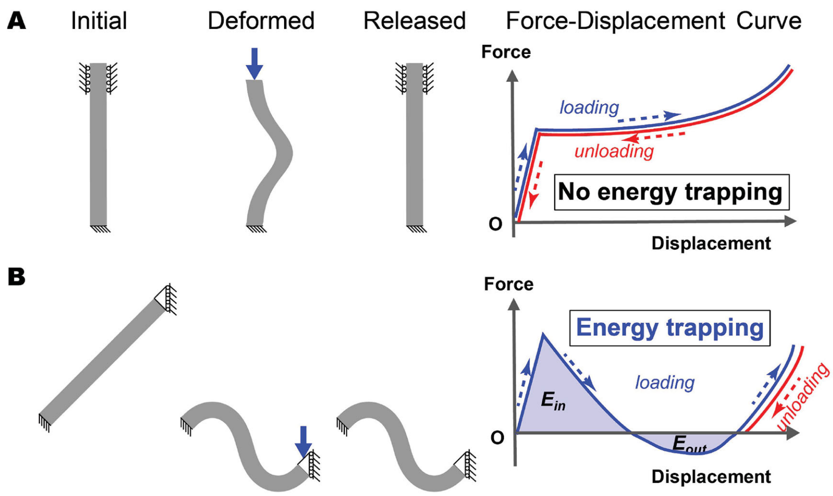

Figure 1. Energy absorption in an elastic beam. a) An elastic beam buckles when axially compressed, yet fully recovers to its initial shape when unloaded. b) A constrained tilted elastic beam may snap between two stable configurations, when one of its ends is moved vertically. In this case, the structure maintains its deformed shape when unloaded. Note: The bistable beams lock in most of the energy inserted into the system during loading ($E_{locked} = E_{in} - E_{out}$). Their initial (undeformed) configuration can be recovered when an amount of energy larger than E_{out} is supplied to the system.

We combined experiments and simulations to systematically investigate the effects of tilting angle θ and beam slenderness t/L (with t and L denoting the thickness and length of the beam, respectively) on the desired energy-trapping response (**Figure 2**). We designed and fabricated a minimal structure consisting of two identical tilted beams, arranged symmetrically to prevent asymmetric deformation, and connected by two stiff horizontal layers (infilled with epoxy) to constrain lateral motion at their ends (Figure 2a,b). We rapidly printed dozens of functional, but minimal, units (each structure requiring only a few minutes to fabricate) (Movie S1, Supporting Information). We specifically explored geometrical parameters (Figure 2a,b) ranging from $\theta \approx 1.5°$ to 70° and $t/L \approx 0.10$ to 0.33 with $L \approx 1$–6 mm. We note that smaller structures could be fabricated using smaller nozzle sizes, while larger structures can be produced via a molding approach (Figures S4 and S5, Supporting Information).

Using FE simulations, we built 2D numerical models of tilted beams characterized by different combinations of θ and t/L and investigated their response under uniaxial compression using the commercial finite element package ABAQUS/Explicit. Each tilted beam is deformed by applying a vertical displacement to the top end, while constraining the motion of both ends in the horizontal direction (see Figure 2c). Quasi-static conditions are ensured by monitoring the kinetic energy and introducing a small damping factor (see Supporting Information). Our experimental and numerical results are in good agreement, as reported in Figure 2d,e. The force–displacement curves shown in Figure 2d clearly indicate that the system's response can be tuned by controlling θ and t/L. For example, we find that the beams snap during compression when (θ, t/L) = (25°, 0.15), but return to their initial (undeformed) configuration after the load is removed (i.e., only the initial configuration is stable). However, for (θ, t/L) = (40°, 0.12) and (60°, 0.14), there is a brief period of tensile reaction force (see region with negative force in the results in Figure 2d), so that the system is bistable and can lock in most of the energy applied during loading. As evident in the right panel of Figure 2c, the beams possess slight fillets at their ends due to a small amount of over-extrusion that occurs at those locations as a result of the finite acceleration of the position stage during 3D printing. This is accounted for by measuring each sample's actual geometrical parameters with a microscope rather than relying on the beam length specified in software.

To further explore the effect of t/L and θ, we carried out a combined numerical and experimental parametric study. The numerical results, summarized in Figure 2e, indicate that by increasing θ, at constant t/L, the response of the beams undergoes several transitions. For low values of θ (i.e., nearly horizontal beam orientation, perpendicular to the loading direction), the system exhibits no instabilities (white region in Figure 2e). Above a critical value of θ, a snap-through instability is triggered (light gray region in Figure 2e), but without bistability. However, in both of these cases, the system returns to its initial configuration upon unloading, i.e., no energy is trapped. If θ is further increased, the beam becomes bistable (colored area in Figure 2e), enabling energy trapping. The geometrical transformation between undeformed and deformed stable states is akin to a phase change, in which the quantity of energy that is trapped depends solely on the net change in deformation, i.e., independent of how the load is applied and of loading history. Finally, if θ is increased above a critical threshold, the snap-through instability is suppressed (gray area in Figure 2e) due to self-contact.

Within the bistable domain, the energy that the system absorbs (E_{in}) increases as a function of both θ and t/L. However, the energy cost for a beam to snap back to its undeformed state (E_{out}) tends to decrease. As a result, it is likely that for large values of θ and t/L (within the bistable region) the system cannot maintain the second stable configuration due to small geometric imperfections or even a time dependency (e.g., viscoelasticity) of the material itself. To design optimal energy trapping beams, one must maximize E_{in} while maintaining E_{out} above a threshold that depends on the environment for which the system is designed. To complement the numerical study, we carried out an experimental parametric study by fabricating minimal structures over the same combinations of θ and t/L. Of particular interest is the transition between the geometries that exhibit bistability and those that merely possess the snap-through instability, but are not bistable. The black dashed lines in Figure 2e indicate the approximate location of this transition, as measured experimentally, which is in good agreement with the numerical results. Discrepancies arise from the fact that structural defects become more important near the transition, since E_{out} is very low there (see Movie S3, Supporting Information). Note, this transition is important, not only because the

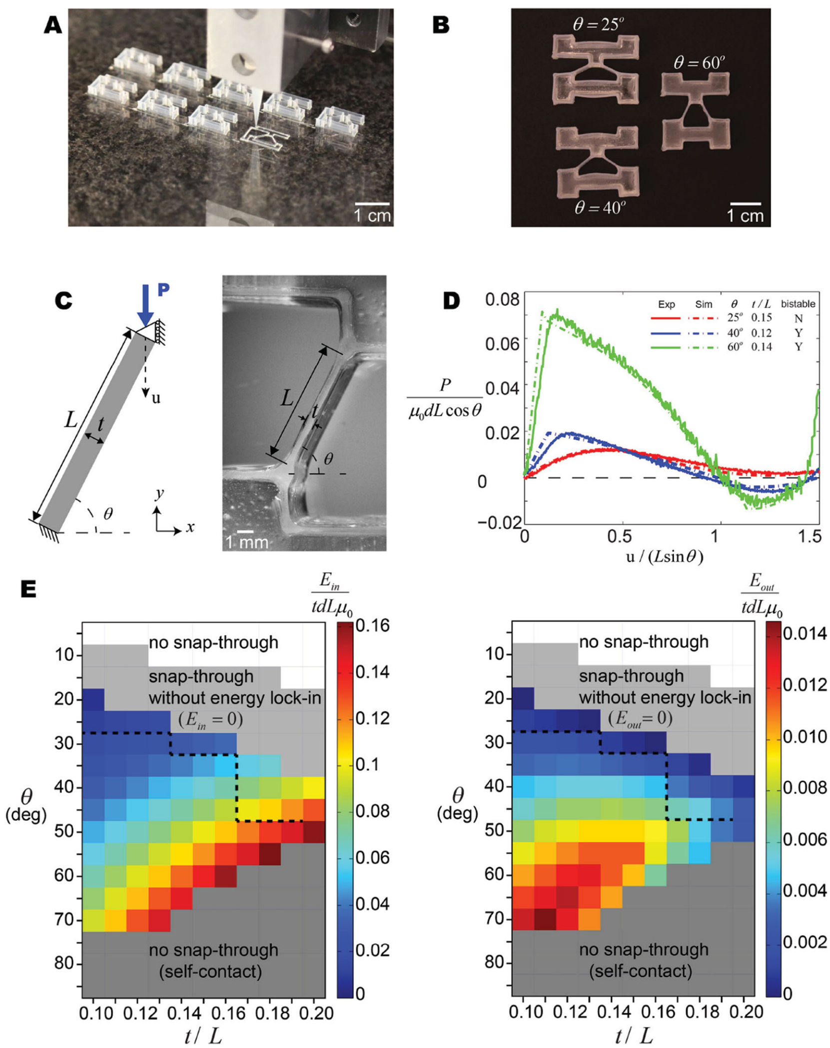

Figure 2. Mechanical response of a constrained, tilted elastic beam. a) Minimal functional structures, each with a unique combination of geometrical parameters, are rapidly printed (150–200 s each) using direct write 3D printing. b) Minimal structures consisting of two identical tilted beams. c) Schematic view showing the 2D model used in our FE simulations (left) and the corresponding beam in the fabricated minimal unit (right). d) Numerical and experimental force–displacement curves for three beams characterized by $(\theta, t/L) = (25°, 0.15)$, $(40°, 0.12)$, $(60°, 0.14)$. The force is normalized by $\mu_0 L\, d \cos\theta$ (d denoting the out-of-plane thickness of the samples), while the displacement is normalized by $L \sin\theta$. e) Effect of θ and t/L on the energy absorbed by the elastic beam (E_{in}) and the energy cost for the beam to snap back to its undeformed configuration (E_{out}). The black dashed lines indicate the experimentally observed transition between the geometries that result in bistability and those that merely possess the snap-through instability, but are not bistable.

bistability enables energy trapping, but also because it could be used in the design of deployable mechanical structures to achieve controlled sequential displacement. Finally, we have also demonstrated that this structural design can be combined with stimuli-responsive materials to produce structures capable of recovering when exposed to an environmental cue (Movie S4, Supporting Information).

Interestingly, the bistable elastic beams can be arranged to form 1D, 2D, or 3D energy-trapping metamaterials (**Figure 3**a). To demonstrate the concept using a system designed to deform uniaxially, we fabricated a 4 × 4 array of minimal units (i.e., two symmetric beams), for a total of 32 tilted beams (Movie S2, Supporting Information). As shown in Figure 3b, if t/L and θ are chosen such that each beam is bistable (in this case, $\theta = 40°$ and $t/L = 0.12$, with $L = 5$ mm), the structure is characterized by multiple stable configurations that can be triggered by applying a compressive force and that are also maintained when the force is removed. In fact, a tensile force needs to be applied to recover the initial shape (Movie S5, Supporting Information). We then characterized the response of the structures under uniaxial compression using a single-axis Instron with a 10 N load cell. As shown in Figure 3c, the force–displacement response is characterized by four similar peaks, each corresponding to the collapse of a row of beams. Since each row is designed with the same geometrical parameters, these peaks occur at a nearly identical force (with small imperfections leading to sequential, rather than simultaneous, collapse of the rows). Remarkably, the magnitude of these peaks for the 4 × 4 structures is in excellent agreement with that observed from the tests of the minimal unit, highlighting the modularity and scalability of this structural motif. When these structures are compressed at different speeds (between 10 and 0.1 mm s^{-1}), their force–displacement curves are shown to be rate independent, and they absorb the same amount of energy per unit mass when fully compressed. Their remarkable insensitivity to loading conditions is due to the fact that all energy inserted into these architected metamaterials is locked-in in the form of elastic strain energy. Therefore, the absorbed energy depends only on the morphological change between the initial (undeformed) state and the final (deformed) state of the beam. We also note that the rate independence demonstrated by the data means that any rate-dependent effects such as material viscoelasticity provide negligible contributions to the energy absorption for the tested regime.

Each of the four layers of the structure in Figure 3 consists of eight tilted beams in parallel, with each of these layers arranged in series. Given this modularity, the total structural response can be predicted using the FE result for the corresponding single beam (see Supporting Information). The agreement between numerical and experimental results (Figure 3d) is excellent, demonstrating that the knowledge of the response of our simple building block is enough to design larger and more complex structures with tailored properties. Moreover, although the results reported in Figure 3b–d are for a structure characterized by $L = 5$ mm, the same strategy can be applied to structures with various length scales (Figure 3e), since we exploit a geometrical

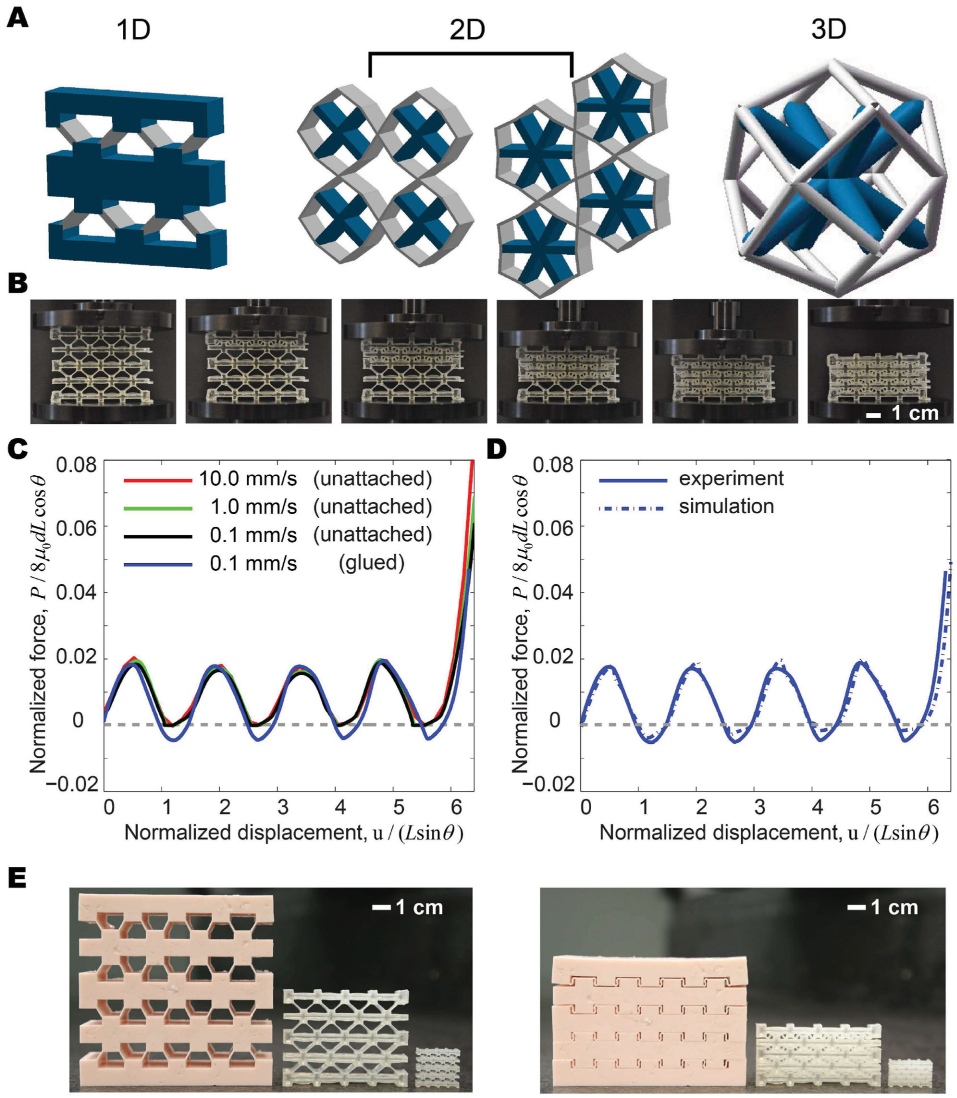

Figure 3. Mechanical response of an elastic multistable structure. a) Schematic views of 1D, 2D, and 3D energy-trapping metamaterials. The bistable beams are colored in gray, while the rigid support structures are colored in blue. b) Sequential images of the multistable structure loaded vertically. The sample retains its deformed shape after unloading. c) Stress–strain curves for the multistable structure at multiple strain rates. The measurements are repeated five times for each strain rate, showing excellent repeatability for a given sample and also between multiple samples with the same geometric properties. d) Comparison between experiments and simulations. The numerical predictions are obtained using the FE results for a single tilted beam with $\theta = 40°$ and $t/L = 0.12$ and by assuming that the structure consists of four layers arranged in series, each with eight tilted beams in parallel. e) Examples of different structures fabricated at different length scales (left: initial; right: deformed).

transformation that is scale-independent (where the continuum assumption holds) and relies solely on the aspect ratio and the orientation angle of the beams. It is also noteworthy that the numerical results match the experimental results closely even though they do not take into account viscoelasticity or other time-dependent phenomena, implying that these effects are negligible in our structures.

We also characterized the ability of the system to provide protection during impact by dropping the samples from different heights, h, while recording the acceleration with a piezoelectric accelerometer (PCB Piezotronics, Inc., Model No. 352C23) attached to their top surface. To investigate the general efficacy of this energy-trapping mechanism, we performed impact tests: (i) on multistable structures in their low-energy, undeformed configuration; (ii) on the same multistable structures in their densified state (effectively, the "control" case, behaving as a block of material); and (iii) on structures with low beam angles ($\theta = 20°$), which possess a snap-through instability, but are not multistable. First, we see that the control sample, which is the densified multistable structure, propagates a very large peak acceleration during impact (gray line in **Figure** 4a,b). As we demonstrate, elastic metamaterials that are based on the snap-through instability, similar to those reported previously,[10] show a reduced peak acceleration (green line) relative to the densified structure. However, by introducing energy trapping via our multistable samples (red line), the peak acceleration

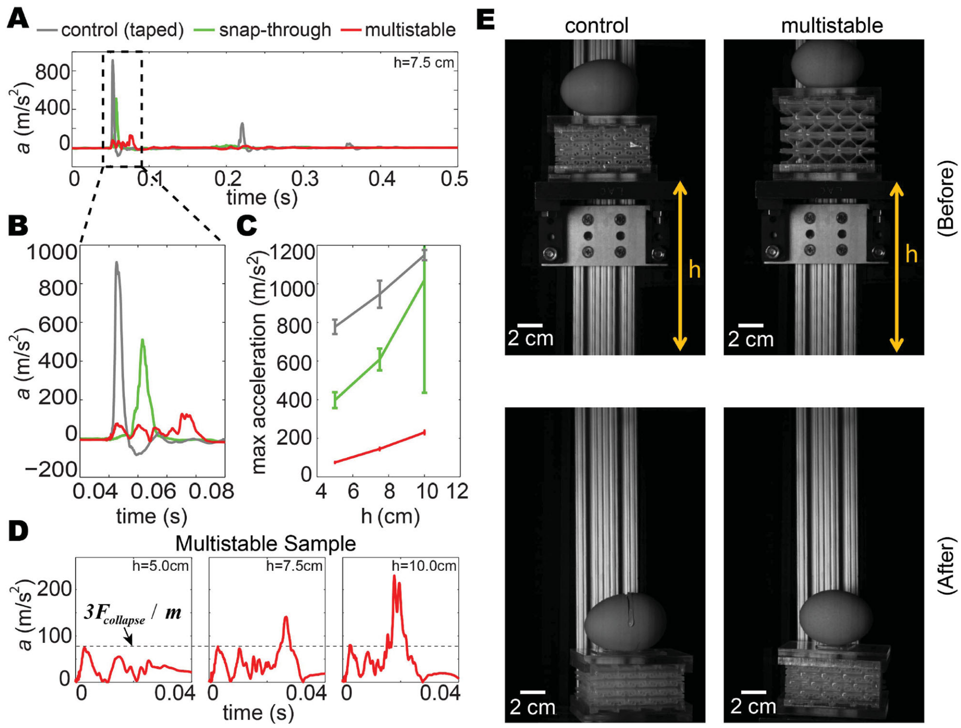

Figure 4. Drop tests. a) Acceleration–time curve for a multistable structure, the corresponding control sample (consisting of the same structures but taped to make all beams intentionally collapsed prior to the drop test), and a structure designed to possess snap-through instabilities but not energy-trapping, with samples dropped from h = 7.5 cm. b) Zoom-in of the acceleration–time curves. c) Peak acceleration amplitude as a function of the dropping height h for the multistable structure, the control sample, and the snap-through sample. The error bars indicate standard deviations from multiple ($N > 5$) measurements. d) Acceleration– time curves for the multistable sample obtained from drop heights of h = 5, 7.5, and 10 cm. The horizontal dotted line indicates the collapse force divided by the mass of the egg for a line of tilted beams. The force is three times larger than that measured in the static compression tests since here we used three identical structures arranged in parallel for the drop tests. e) Drop of multistable and control samples with raw eggs attached to their top from h = 12.5 cm. The eggs attached to the multistable structures survive, while those on the control samples break upon impact.

during impact and the structure's protective capability are improved by an order of magnitude for a given mass of material (Figure 4a,b).

Further comparison between the multistable, snap-through, and control samples clearly shows the ability of the energy-trapping beams to improve impact performance, yielding up to an order of magnitude reduction in peak acceleration amplitude when h was varied between 5 and 10 cm (Figure 4c). For samples designed to possess the snap-through instability without energy trapping (θ = 20° and t/L = 0.11), significantly less energy is absorbed despite having very similar relative density to the energy-trapping structures. The simulations predict no energy absorption for the samples without energy trapping, since material dissipation is not accounted for; however, there is a small amount of energy absorption in the experiments because of viscoelasticity.

The acceleration–time curve for multistable samples is characterized by four peaks at $a \approx 80$ m s^{-2}, each corresponding to the collapse of a line of beams. This acceleration corresponds to a force $F = m \times a = 0.125$ kg $\times$ 80 m s^{-2} = 10 N ($m = 0.125$ kg being the combined mass of the egg and acrylic fixture we placed on the top of the energy absorbing structures), which is in excellent agreement with the collapse force measured during the quasistatic compression of the structures (see Supporting Information). This remarkable result further highlights the rate-independent mechanism, since the collapse force during impact would not typically be expected to be the same as during quasistatic compression.[26] As the drop height h is increased (Figure 4d), eventually the kinetic energy of the structure immediately prior to impact exceeds the cumulative absorptive potential of the snapping beams in all four rows. As a result, for high enough h (7.5 cm and above in this case) an additional acceleration peak emerges, corresponding to loading of the densified structure after all four rows of beams have fully collapsed. We can optimize the design for a given application by maximizing the energy dissipated during collapse of the beams subject to the constraint that the acceleration remains below a particular damaging acceleration. This can be controlled by varying the structural parameters (θ and t/L) as well as the out-of-plane thickness of the structure.

The energy-trapping capability of our multistable, architected materials could be beneficial for protecting an object and/or a person from impact. To illustrate this, we dropped multistable and control samples with raw eggs attached to their top surfaces. As shown in Figure 4e, the eggs attached to the energy-absorbing structure remain intact, while those attached to the control samples break upon impact (Movie S6, Supporting Information). Importantly, after the impact, these multistable architected materials can be reused, maintaining the same energy absorption characteristics regardless of loading history.

In summary, by combining numerical calculations and 3D printing, we have developed fully elastic and reusable energy-trapping architected materials based on localized locking-in of strain energy in tilted elastic beams. Our strategy offers several advantages; it can be applied to structures with various length scales (from micro to macro) and provides a simple modular design scheme, so that the mechanical response can be tuned by controlling geometric parameters guided by a "phase diagram." Moreover, the loading process is fully reversible, allowing the structures to be consistently reused many times, with the energy absorption unaffected by loading rate or history. Since the quantity of energy that is trapped in these metamaterials depends solely on the morphological change between the initial (undeformed) and final (deformed) stable states of the elastic beams (for a given material), their response is highly predictable for a wide variety of loading conditions. The structural energy-trapping mechanism could also be combined with more traditional, material-dependent dissipative mechanisms, such as viscoelasticity, to enhance the total protective capabilities of a system by harnessing multiple dissipation or absorption mechanisms simultaneously. Our findings open new opportunities for designing energy-absorbing materials for applications including reusable personnel protection, crash mitigation in automobiles and aircraft, and protective packaging of delicate components.

Supporting Information

Supporting Information is available from the Wiley Online Library or from the author.

Acknowledgements

S.S., S.H.K., and J.R.R. contributed equally to this work. This work was supported by NSF Harvard MRSEC through Grant Nos. DMR-1420570 and CMMI-1149456 (CAREER) and by the Wyss Institute through the Seed Grant Program. K.B. acknowledges start-up funds from the Harvard School of Engineering and Applied Sciences and the support of the Kavli Institute at Harvard University. The authors would also like to thank Dr. Lori Sanders for help with photography and Mr. Qi Jian Lim and Mr. Sijie Sun for help with experiments. The authors declare that they have no competing financial interests.

Received: April 10, 2015
Revised: May 13, 2015
Published online: June 18, 2015

[1] L. J. Gibson, M. F. Ashby, *Cellular Solids: Structure and Properties* Pergamon Press, New York **1988**.
[2] S. D. Papka, S. Kyriakides, *J. Mech. Phys. Solids* **1994**, *42*, 1499.
[3] A. Pugsley, M. Macaulay, *Q. J. Mech. Appl. Math.* **1960**, *13*, 1.
[4] S. R. Reid, *Int. J. Mech. Sci.* **1993**, *35*, 1035.
[5] H. G. Tattersall, G. Tappin, *J. Mater. Sci.* **1966**, *1*, 296.
[6] M. A. Dawson, G. H. McKinley, L. J. Gibson, *J. Appl. Mech.* **2008**, *75*, 041015.
[7] L. Gong, S. Kyriakides, W.-Y. Jang, *Int. J. Solids Struct.* **2005**, *42*, 1355.
[8] B. Florijn, C. Coulais, M. van Hecke, *Phys. Rev. Lett.* **2014**, *113*, 175503.
[9] L. R. Meza, S. Das, J. R. Greer, *Science* **2014**, *345*, 1322.
[10] D. M. Correa, T. Klatt, S. Cortes, M. Haberman, D. Kovar, C. Seepersad, *Rapid Prototyping J.* **2015**, *21*, 193.
[11] L. Salari-Sharif, T. Schaedler, L. Valdevit, *J. Mater. Res.* **2014**, *29*, 1755.
[12] J. A. Lewis, *Adv. Funct. Mater.* **2006**, *16*, 2193.
[13] S. Guest, S. Pellegrino, *Proc. R. Soc. London A* **2006**, *462*, 839.
[14] A. Pandey, D. E. Moulton, D. Vella, D. P. Holmes, *Europhys. Lett.* **2014**, *105*, 24001.
[15] F. Fraternali, T. Blesgen, A. Amendola, C. Daraio, *J. Mech. Phys. Solids* **2011**, *59*, 89.
[16] Y. Forterre, J. M. Skotheim, J. Dumais, L. Mahadevan, *Nature* **2005**, *433*, 421.
[17] D. Holmes, A. Crosby, *Adv. Mater.* **2007**, *19*, 3589.
[18] Q. Guo, H. Zheng, W. Chen, Z. Chen, *Biomed. Mater. Eng.* **2014**, *24*, 557.
[19] Z. P. Bazant, L. Cedolin, *Stability of Structures: Elastic, Inelastic, Fracture, and Damage Theories* Oxford University Press, New York **1991**.
[20] S. Timoshenko, *J. Appl. Mech.* **1935**, *2*, 17C20.
[21] A. Fargette, S. Neukirch, A. Antkowiak, *Phys. Rev. Lett.* **2014**, *112*, 137802.
[22] A. Pandey, D. Moulton, D. Vella, D. Holmes, *Europhys. Lett.* **2014**, *105*, 24001.
[23] G. M. Gratson, M. Xu, J. A. Lewis, *Nature* **2004**, *428*, 386.
[24] J. E. Smay, J. Cesarano III, J. A. Lewis, *Langmuir* **2002**, *18*, 5429.
[25] B. Y. Ahn, E. B. Duoss, M. J. Motala, X. Guo, S.-I. Park, Y. Xiong, J. Yoon, R. Nuzzo, J. A. Rogers, J. A. Lewis, *Science* **2009**, *323*, 1590.
[26] M. Zupan, C. Chen, N. A. Fleck, *Int. J. Mech. Sci.* **2003**, *45*, 851.

